Rev.Adv.Mater.Sci. 15(2007) 1-9

# SYNTHESIS OF AN ULTRA-THIN PALLADIUM MEMBRANE FOR HYDROGEN EXTRACTION

**Zhongliang Shi and Jerzy A. Szpunar**

Department of Mining, Metals and Materials Engineering, McGill University, 3610 University Street, M.H. Wong Building, Montreal, QC, H3A 2B2, Canada

*Received: January 22, 2007*

**Abstract.** Based on the observation of the microstructure of palladium deposited on a porous stainless steel surface using an electroless process, we find that the palladium membrane is made of nanoparticles and its thickness is directly dependent on the size of the nanoparticles. The size of palladium nanoparticles can be effectively controlled by concentration of $PdCl_2$ in the plating solution. The higher concentration of $PdCl_2$ in the plating bath will result in a smaller size of palladium particles deposited on the substrate. The smaller the size of palladium nanoparticles is generated from the solution, the thinner the dense palladium membrane is built. The result obtained from hydrogen permeation through the ultra-thin palladium membrane having a thickness of 400 nm demonstrates that this ultra-thin membrane is solid and it can be used at the temperature of 550 °C and hydrogen pressure difference of 50 psi. These experimental results will allow optimizing the design of an ultra-thin palladium membrane for hydrogen extraction.

## 1. INTRODUCTION

Global interest in the development of a “hydrogen economy” and an associated demand for hydrogen as a source of clean energy has led to the development of new materials and methods for hydrogen generation, storage, separation and sensing [1]. So far, palladium and palladium alloys are regarded as the most important materials for high quality hydrogen extraction from a mixture of gases. The interaction between palladium and hydrogen has been studied extensively and palladium membranes have been widely applied for hydrogenation catalysts in chemical engineering because palladium absorbs and adsorbs hydrogen easily. Palladium membranes have high hydrogen permeability, good chemical compatibility and excellent hydrogen selectivity [2-8]. They are usually built by electroless, electrochemical and sputtering depositions. Most efforts have been focused on the reduction of the membrane thickness in order to maximize hydrogen permeability and reduce the membrane cost [9-11]. No matter what kind of process is employed to build palladium membrane, the membrane should be dense enough to allow hydrogen permeation and block the other gases. As it is well known, the mechanism of hydrogen permeation through a palladium membrane involves 3 steps, such as dissociative adsorption, recombinative desorption at the membrane surface and diffusion through the membrane. The flux of hydrogen through a membrane is generally determined by its thickness. However, the fabrication of a dense and ultra-thin palladium membrane is quite challenging and attracts new application in microdevices [12,13]. The purpose in this paper is to observe how palladium is deposited on the stain-

Corresponding author: Zhongliang Shi, e-mail: zhongliang.shi@mail.mcgill.ca

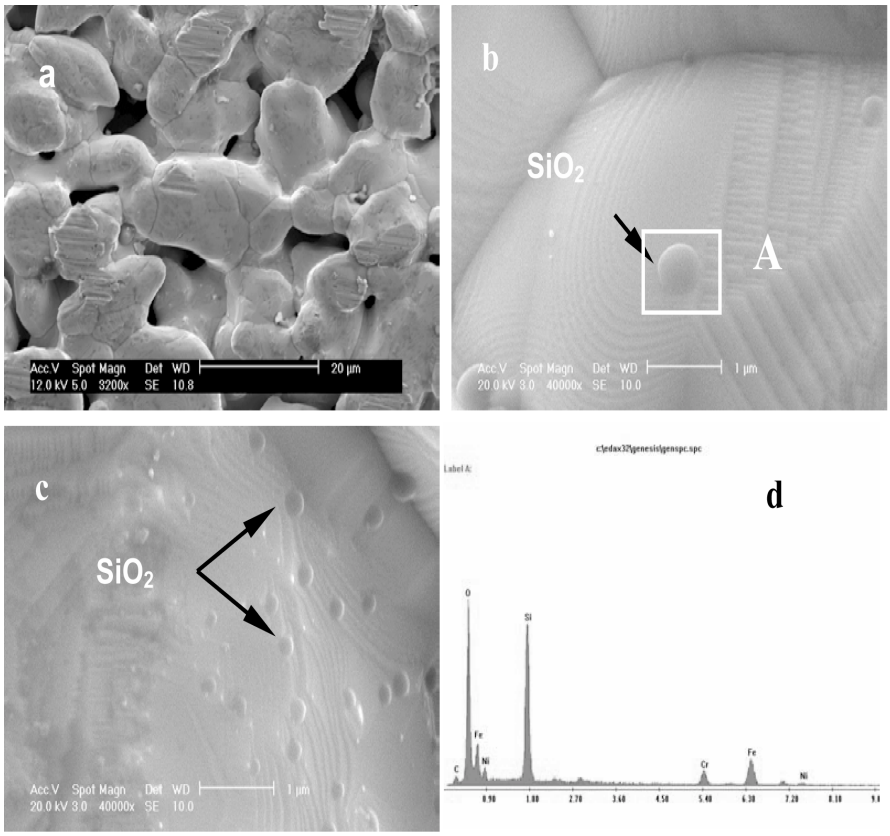


**Fig. 1.** SEM micrographs (a-c) showing the surface of the porous stainless steel substrate, (d) energy-dispersive X-ray spectrum from the marked area A that indicates the presence of $SiO_2$-riched particle at the substrate surface.

less steel substrate at different concentrations of $PdCl_2$ in the plating bath, to investigate how the dense membrane is built and to explain how an ultra-thin membrane can be fabricated. These experimental results are beneficial to the design and fabrication of an ultra-thin palladium membrane for engineering applications.

## 2. EXPERIMENTAL

In this research, a 0.2 μm grade porous 316L stainless steel plate, purchased from Mott Metallurgical Corporation was used as a substrate to deposit a palladium membrane. This substrate having good mechanical strength and inter-connected porosity was fabricated by powder metallurgical process. These interconnected porosities are defined as pores that are connected to the surfaces of the component and allow fluid flow from one side to the other. The porosity of this substrate is defined as a 0.2 μm grade that means over 95% of 0.2 μm size particles and fluids are rejected by this support during filtering. The substrate samples have the sizes of 20 mm x 20 mm and ∅ 45 mm. The small square substrate samples are used to char-

**Table 1.** The composition of the electroless plating bath and experimental parameters [14,15].

| Component | Composition and experimental parameters |
|---|---|
| $PdCl_2$ | 1.8~2 g/l, 2.4 g/l, 3.0 g/l, 4.2 g/l |
| $Na_2EDTA.2H_2O$ | 40.1 g/l |
| $NH_3$ (28%) | 198 ml/l |
| $N_2H_4$ (1M) | 5.6 ml/l |
| pH | 10 ~ 10.4 |
| Temperature (°C) | 60 |

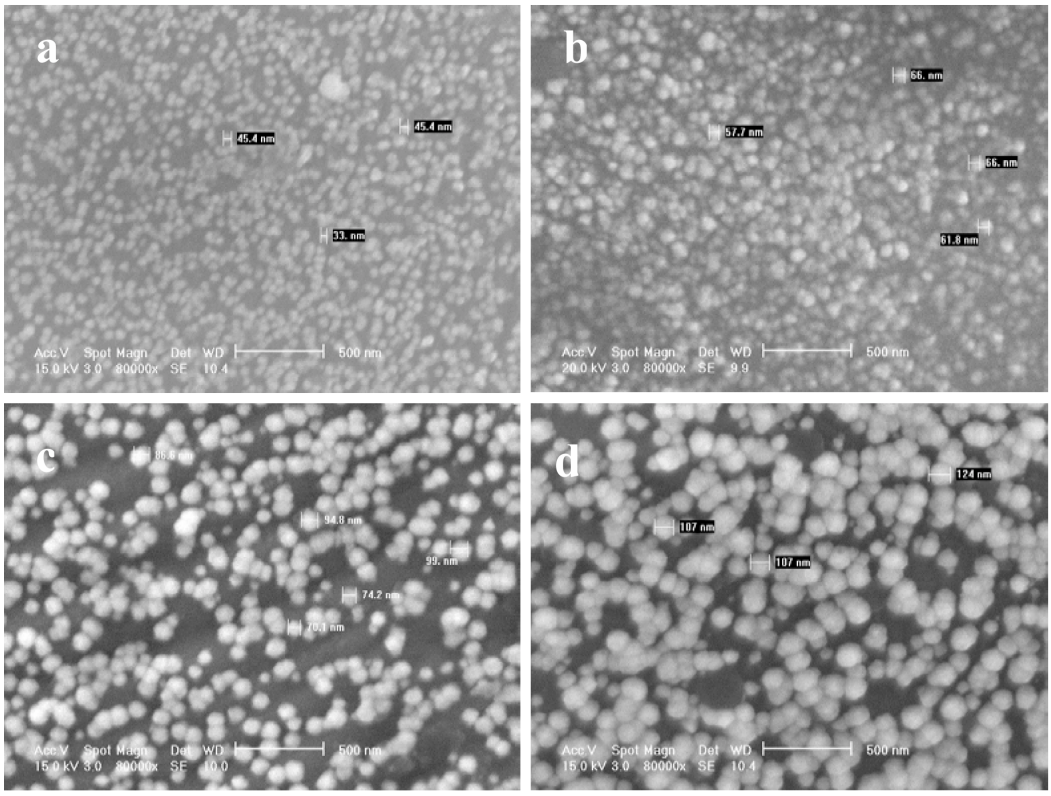


**Fig. 2.** SEM micrographs showing palladium nanoparticles deposited on the surface of a stainless steel substrate at different concentration of $PdCl_2$ in the plating bath under the same time of 150 s (a) The size: 30 ~ 50 nm, $C_{PdCl2}$: 4.2 g/l; (b) The size: 50 ~ 70 nm, $C_{PdCl2}$: 3 g/l; (c) The size: 70 ~ 100 nm, $C_{PdCl2}$: 2.4 g/l; (d) The size: 100 ~ 130 nm, $C_{PdCl2}$:1.8~2 g/l.

acterize the microstructure of the palladium deposits in the initial stages at different concentrations of $PdCl_2$ in the plating solution. The substrate samples having a diameter of 45 mm are used to deposit palladium membranes for hydrogen permeation tests. They were cleaned in an ultrasonic bath with acetone for 15 min. Then, their surfaces were activated and rinsed with deionized water. After such treatments, these substrate samples were transferred into the electroless plating bath with different concentrations of $PdCl_2$ for the deposition of palladium. The deposition time was from 30 s to 30 min at a constant temperature of 60 °C. The detailed palladium plating baths preparation using hydrazine as a reducing agent is described in Table 1. Microstructural characteristics of palladium membranes were analyzed using a PHILIPS XL30 FE SEM (Field Emission Scanning Electron Microscopy) equipped with an EDS (Energy Dispersive Spectroscopy, GENESIS 2000 X-ray Microanalysis System). The gas-tightness of the membranes was examined and no leakage was detected with nitrogen gas at the pressure of 50 psi from room temperature to 550 °C. The hydrogen permeation tests for the deposited membranes were carried out in a permeation cell at the temperature from 25 to 550 °C and a hydrogen pressure difference from 20 psi to 50 psi. The measurement of the hydrogen flux using a soap bubble meter was at the temperature from 300 to 550 °C. The experimental apparatus used for the gas permeation tests was similar to the one described elsewhere [14].

## 3. RESULTS AND DISCUSSION

Fig. 1 shows the microstructure of a porous stainless steel substrate. It can be seen that some spherical phases are observed at the surface of

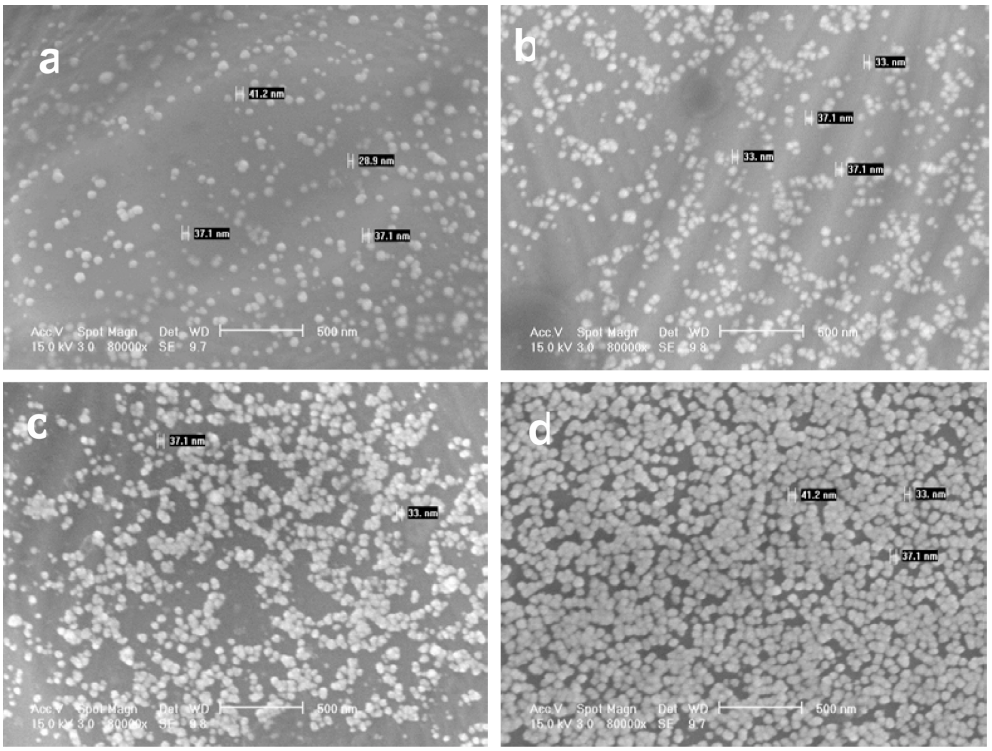


**Fig. 3.** SEM micrographs showing palladium nanoparticles deposited on the surface of stainless steel substrate at the $PdCl_2$ concentration of 4.2 g/l in the plating bath. The deposition time: (a) 30 s, (b) 60 s, (c) 75 s, and (d) 150 s.

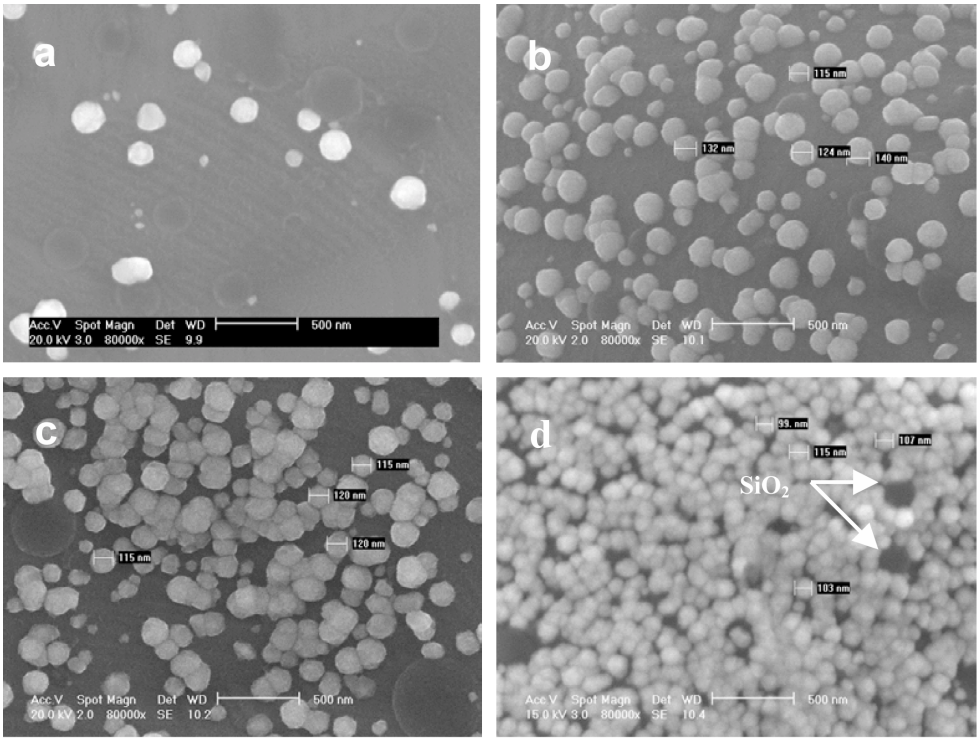


**Fig. 4.** SEM micrographs showing palladium nanoparticles deposited on the surface of a stainless steel substrate with $PdCl_2$ concentration of 1.8~2 g/l in the plating bath. The deposition time: (a) 30 s, (b) 90 s, (c) 120 s, and (d) 300 s.

the substrate, as shown in Figs. 1b and 1c. These spherical particles, analyzed by EDS in Fig. 1d, are $SiO_2$ inclusions that are most likely generated from soluble silicate used as inorganic binders during powder metallurgical process. The size of the $SiO_2$ inclusions ranges from 150 to 600 nm. Their existence at surface of the substrate was used to estimate the thickness of palladium deposits at the initial stages of deposition.

SEM micrographs in Figs. 2-4 illustrate palladium nanoparticles deposited on the stainless steel substrate at the time from 30 s to 300 s and at different concentrations of $PdCl_2$ in the plating bath. One can see that the deposited palladium nanoparticles are distributed at the substrate randomly and the particle size is varying with the concentrations of $PdCl_2$ in the plating bath. The higher the concentration of $PdCl_2$ in the plating bath is, the smaller the deposited palladium nanoparticles are, as illustrated in Fig. 2. Comparing the size of palladium nanoparticles deposited on the steel substrate in different concentrations of $PdCl_2$ but at the same deposition time of 150 s, we can see that the size of deposited palladium nanoparticles changes from 30~50 nm to 50~70 nm when the concentration of $PdCl_2$ in the plating bath is reduced from 4.2 g/l to 3 g/l, as shown in Figs. 2a and 2b. When the concentration of $PdCl_2$ in the plating solution changes from 2.4 g/l to 1.8~2.0 g/l, the size of deposited palladium nanoparticles increases from 70~100 nm to 100~130 nm, as shown in Figs. 2c and 2d. However, the size of palladium nanoparticles does not change with the extension of deposition time at the same concentration of $PdCl_2$ but depends only on the concentration of $PdCl_2$ in the plating solution, as shown in Figs. 3 and 4. The size of most palladium nanoparticles in Figs. 2a and 3 is in the range of 30~50 nm at the deposition time from 30 s to 150 s. When the concentration of $PdCl_2$ in the plating bath is reduced to 1.8~2 g/l, the size of most deposited palladium nanoparticles is in the range of 100~130 nm, as shown in Fig. 4. However, the number of deposited palladium nanoparticles increases with deposition time, as shown in Figs. 3 and 4. This experimental result is different from published reports that claim that the size of deposited nanoparticles is increasing with the deposition time [15-17]. In order to verify this experimental phenomenon, we also observed the deposition of palladium on the stainless steel substrate within 30 s and found that the number of palladium nanoparticles is directly related to the deposition time but the size of palladium nanoparticles keeps constant at the same concentration of $PdCl_2$ in the plating solution. The deposition of palladium takes place according to the equation of autocatalytic reaction:

$$2Pd[NH_4]^{2+} + N_2H_4 + 4\,OH^{-1} \rightarrow$$
$$2Pd + N_2 + 4\,H_2O + 8\,NH_3$$

When the size of palladium clusters becomes a critical one in a homogeneous plating solution, they will generate from the plating solution and be deposited on the heterogeneous steel substrate forming nanoparticles. The critical size of clusters is determined by the concentration of $PdCl_2$ in the plating bath. Therefore, we can conclude that the deposition of palladium on the stainless steel substrate is controlled by the nucleation at the substrate surface and their growth is limited. As elucidated in the literature [18], in order to obtain nanosize metallic particles, a high supersaturation concentration is often required, which are best achieved when starting with non-complexed, highly reactive metallic species and very strong reducing agents. If the fraction of atoms consumed in the nucleation step is high, the increase in particle size due to the diffusional growth that immediately follows the nucleation burst is drastically limited and the particles are only slightly larger than the nuclei. Based on our experiments, when the concentration of $PdCl_2$ in the plating solution increases, the deposition and nucleation of palladium on the substrate is fast and all nuclei form instantaneously and the subsequent growth of palladium deposits is limited. The size of deposited particles is obviously reduced with increasing the concentration of $PdCl_2$ in the plating bath. Therefore, the size of palladium nanoparticles deposited on the steel substrate in the initial stages can be controlled by the concentration of $PdCl_2$ in the plating bath. The formation mechanism of palladium nanoparticles generated from the autocatalytic reaction and their size control are being further investigated.

Fig. 4d shows that most of the substrate is covered by palladium nanoparticles except some small areas occupied by $SiO_2$ inclusions. Based on the observation of palladium deposits after 300 s, we can conclude that an ultra-thin palladium membrane is built at the substrate surface. This membrane has the thickness of a few nanoparticle layers and some small areas containing $SiO_2$ inclusions are not fully covered by palladium nanoparticles. Palladium nanoparticles are not deposited at the surface of $SiO_2$ inclusions because these inclusions are not conductive and there is

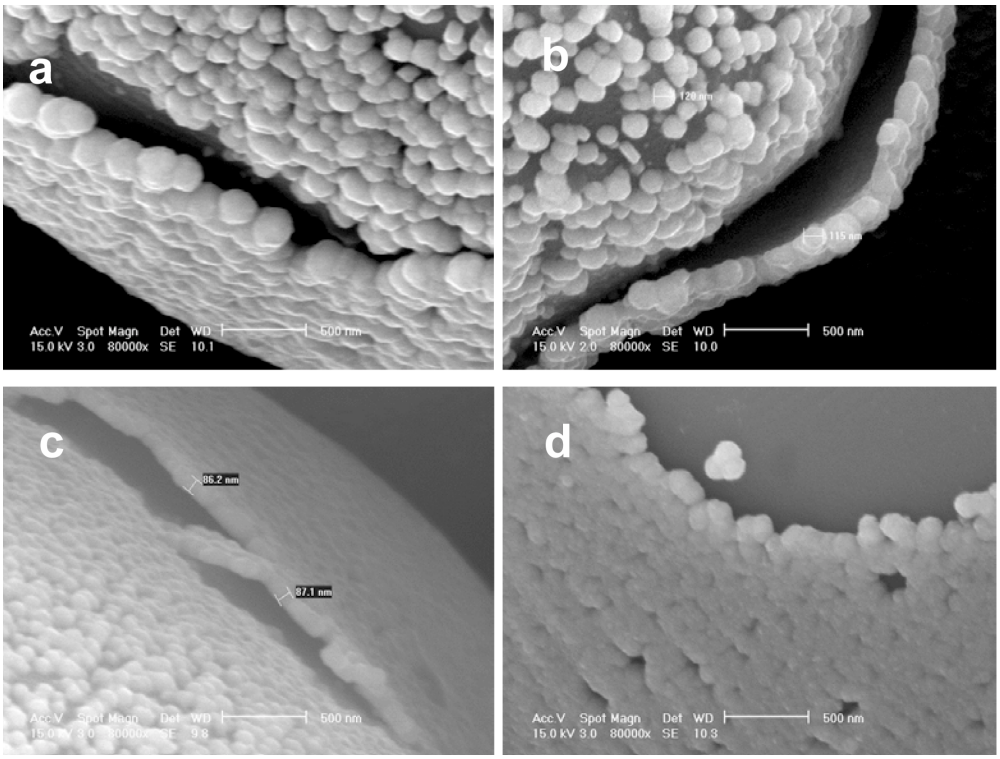


**Fig. 5.** SEM micrographs showing nanoparticle-monolayer membranes deposited on the substrate surface (a, b) The size: 100 ~ 130 nm, time: 120 s; concentration of $PdCl_2$: 1.8~2 g/l, (c, d) The size: 70 ~ 100 nm, time: 120 s, concentration of $PdCl_2$: 2.4 g/l.

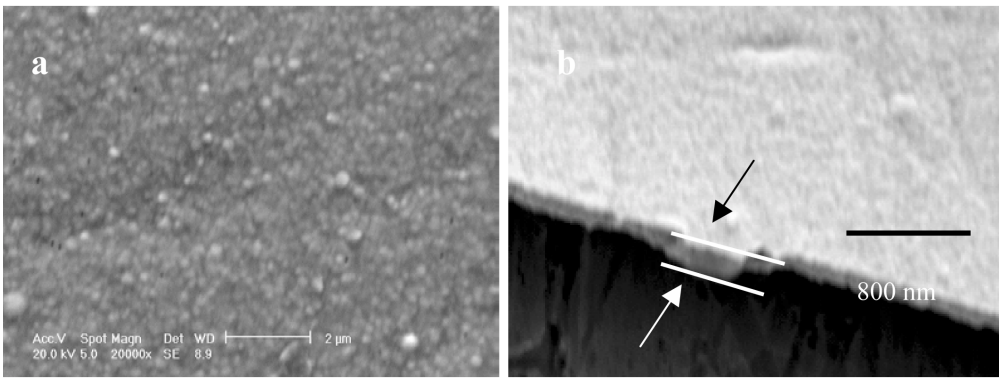


**Fig. 6.** Microstructure of a palladium membrane deposited on a modified porous stainless steel substrate by electroless deposition (The deposition time: 30 min; concentration of $PdCl_2$ in plating bath: 1.8~2 g/l).

no electronic exchange at their surfaces during the autocatalytic reaction. As illustrated in Figs. 1b and 1c, the thickness of the palladium membrane can be estimated based on the size of $SiO_2$ inclusions.

SEM micrographs in Figs. 5a-5d show a nanoparticle-monolayer palladium membrane made of nanoparticles deposited on the wall of a pore area. The thickness of the palladium membrane in this case, as shown in Figs. 5a and 5b, is around 100 ~ 130 nm which is the same as the size of palladium nanoparticles in Figs. 2d and 4. When the concentration of $PdCl_2$ in the plating solution increases to 2.4 g/l, the thickness of palladium layer will decrease to 70~100 nm, as shown in Figs. 5c and 5d. This palladium nanoparticle monolayer membrane is dense and palladium nanoparticles are close-packed and well-organized. These nanoparticles are amalgamated in one plane

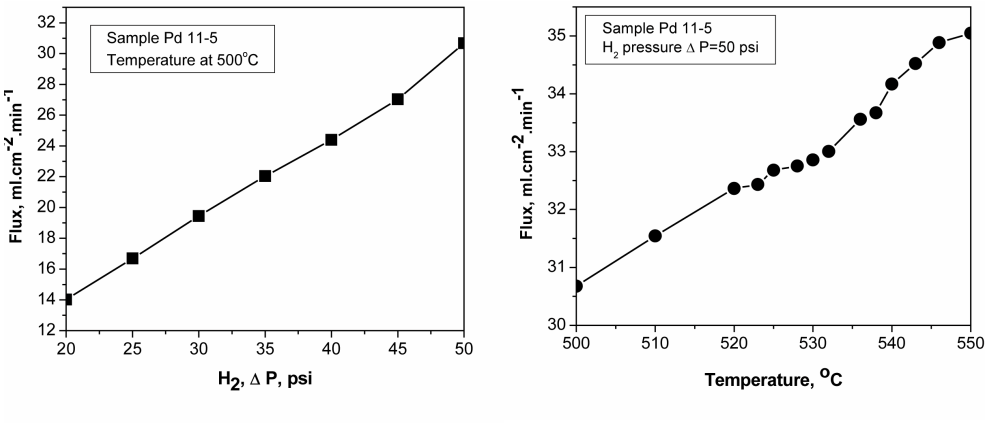


(a) (b)

**Fig. 7.** Hydrogen flux vs. hydrogen pressure difference (a) and temperature (b).

and may then fuse together to lower surface free energy. Such a monolayer membrane made of nanoparticles may not be dense enough for hydrogen purification. However, the membrane assembled by a few monolayers should be dense enough for the extraction of hydrogen from a gas mixture.

Figs. 6a and 6b illustrates the microstructures of the surface and cross-section of an ultra-thin palladium membrane deposited on a modified porous stainless steel substrate at the time of 30 min and $PdCl_2$ concentration of 1.8~2 g/l in the plating bath. This membrane having the diameter of ∅ 45 mm was used for hydrogen permeation tests. The tested area for hydrogen permeation at this membrane was 42 mm in diameter. The membrane was solid and dense because there was no leakage detected when the gas tightness of the membrane was examined using nitrogen gas at gas pressure difference of 50 psi (3.4 atm.). This test was carried from room temperature to 550 °C. The membrane thickness was about 300~400 nm as shown in Fig. 6b. The flux of hydrogen through this membrane is a function of hydrogen pressure and test temperature, as shown in Figs. 7a and 7b. One can see that the flux of hydrogen through the membrane linearly rises with increasing the temperature and hydrogen pressure.

Since the palladium membrane is essentially made of nanoparticles, one can assure that palladium nanoparticles having the same size are packed in a sample geometrical array, as shown in Fig. 8a and the thickness of the membrane is $T$ (nm), where $n$ is the number of nanoparticle monolayer, and $R$ is the radius of palladium nanoparticles. The relationship between $T$, $n$ and $R$ can be expressed in the equations (1) and (2) according to Figs. 8b and 8c.

$$T = 2R + (n-2) \times 0.41R\,, \tag{1}$$

$$n = (T / R - 1172) / 0.414\,. \tag{2}$$

If the thickness of an ultra-thin palladium membrane is 200 nm, the number of layers as function of the radius of nanoparticles is illustrated in Fig. 8d. For example, when the radius of nanoparticle is 10 nm, the membrane having the thickness of 200 nm is approximately assembled by 45 nanoparticle monolayers. As the size of palladium nanoparticles in Figs. 2d and 4 is about 100~130 nm, the membrane was built on the same experimental conditions and its thickness ranges from 300 nm to 400 nm. Thus, according to the Eq. (2), this membrane should be built from about 12 nanoparticle monolayers. The experimental results obtained from hydrogen permeation tests demonstrate that this membrane is solid and dense, and it can be used for hydrogen extraction up to the temperature of 550 °C and hydrogen pressure difference of 50 psi. Therefore, based on these experimental results, the required thickness of an ultra-thin palladium

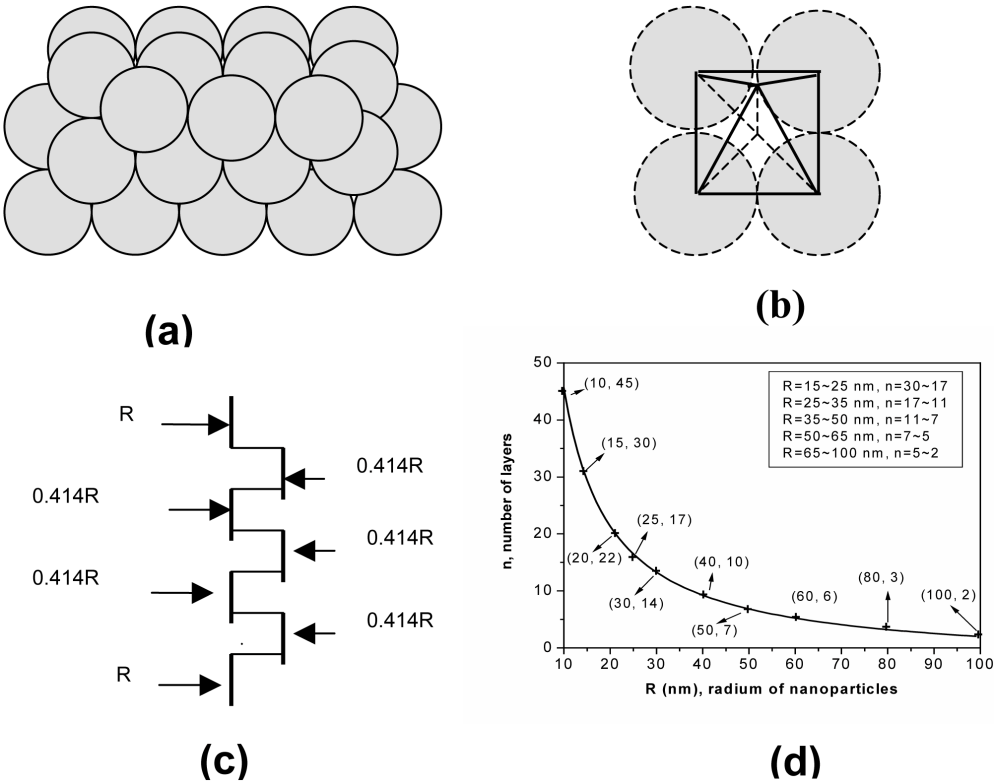


**Fig. 8.** Schematic illustrations of particles packing (a-c) and the relationship between the radius of nanoparticles and the number of nanoparticle layers (d) when the membrane thickness is 200 nm.

membrane can be designed and realized through the control of the concentration of $PdCl_2$ in the plating bath.

## 4. CONCLUSIONS

The observation of palladium deposition on a porous stainless steel substrate by an electroless process shows that the membrane is built from nanoparticles. The size of the palladium nanoparticles can be effectively controlled by changing the concentration of $PdCl_2$ in the plating solution. The thickness of an ultra-thin palladium membrane is directly determined by the diameter of palladium nanoparticles. The smaller the size of palladium nanoparticles is deposited, the thinner the dense palladium membrane will be built. The experimental data obtained from the ultra-thin palladium membrane having the thickness of 300 ~ 400 nm shows that this membrane is dense and it can be used at the temperatures of 550 °C and hydrogen pressure difference of 50 psi. This result will lead to optimize the design of an ultra-thin palladium membrane and to control effectively its fabricated process in micro-devices application.

## REFERENCES

[1] C.J.M. van Rijn, *Nano and Micro engineered membrane technology, Membrane Science and Technology Series, 10* (ELSEVIER, 2004).

[2] T. Mitsui, M. K. Rose, E. Fomin, D. F. Ogletree and M. Salmeron // *Nature* **422** (2003) 705.

[3] F. Favier, E.C. Walter, M.P. Zach, T. Benter and R.M. Penner // *Science* **293** (2001) 2227.

[4] B. L. French, Luke M. Davis, E. S. Munzinger, J. W. J. Slavin, P. C. Christy, D. W. Thompson and R. E. Southward // *Chem. Mater.* **17** (2005) 2091.

[5] S. Yoda, A. Hasegawa, H. Suda, Y. Uchimaru, K. Haraya, T. Tsuji and K. Otake // *Chem. Mater*. **16** (2004) 2363.

[6] Z. Shi, S. Wu, J.A. Szpunar and M. Roshd // *J. Membr. Sci.* **280** (2006) 705.
[7] C. Sachs, A. Pundt, R. Kirchheim, M. Winter, M. T. Reetz and D. Fritsch // *Phys. Rev. B* **64** (2001) 075408.
[8] S. Csonka, A. Halbritter, G. Mihaly, O. I. Shklyarevskii, S. Speller and H. van Kempen // *Phys. Rev. Lett.* **93** (2004) 016802.
[9] K.S. Rothenberger, A.V. Cugini, B.H. Howard, R.P. Killmeyer, M.V. Ciocco, B.D. Morreale, R.M. Enick, F. Bustamante, I.P. Mardilovich and Y.H. Ma // *J. Membr. Sci.* **244** (2004) 55.
[10] A. Johansson, J. Lu, J.-O.Carlsson and M. Boman // *J. Appl. Phys.* **96** (2004) 5189.
[11] D.-W Lee, Y.-G. Lee, S.-E Nam, S.-K. Ihm and K.-H. Lee // *J. Membr. Sci.* **220** (2003) 137.
[12] F.C. Gielens, H.D. Tong, C.J.M. van Rijn, M.A.G. Vorstman and J.T.F. Keurentjes // *J. Membr. Sci.* **243** (2004) 203.
[13] S.V. Karnik, M.K. Hatalis and M.V. Kothare // *J. of Microelectromechanical Systems* **12** (2003) 93.
[14] S.-E. Nam, S.-H. Lee and K.-H. Lee // *J. Membr. Sci.* **153** (1999) 163.
[15] J. L. Fransaer and R. M. Penner // *J. Phys. Chem. B* **103** (1999) 7643.
[16] T. Hirsch, M. Zharnikov, A. Shaporenko, J. Stahl, D. Weiss, O. S. Wolfbeis and V. M. Mirsky // *Angew. Chem. Int. Ed.* **44** (2005) 6775.
[17] Y. Fu, L. Zhang and J. Zheng // *J Nanosci Nanotechnol.* **5** (2005) 558.
[18] D.V. Goia // *J. Mater. Chem.* **14** (2004) 451.